aerospace

MDPI

Article

Conceptual Design of Metal Hydride Cartridges with Systematic Alloy Selection and Sizing Guidelines for Boil-Off-Gas Recovery from Liquid Hydrogen †

Florian Franke * and Stefan Kazula

Institute of Electrified Aero Engines, German Aerospace Center (DLR), 03046 Cottbus, Germany
* Correspondence: florian.franke@dlr.de
† This article is a revised and expanded version of a paper published in Franke, F.; Kazula, S. Conceptual Design of a Metal Hydride Cartridge for the Recovery of Gaseous Boil-off Losses from Liquid Hydrogen Tanks. In Proceedings of the 15th EASN International Conference, Madrid, Spain, 14–17 October 2025.

Abstract

Hydrogen has huge potential for sustainable future industries, but the formation of hydrogen boil-off gas (BOG) is a main drawback of liquid hydrogen (LH2) applications as BOG venting raises safety issues and leads to significant hydrogen loss. A promising approach for BOG recovery is a system with exchangeable cartridges filled with metal hydride (MH). Previous studies focus on the macroscopic level of the interaction between the cartridges with the boil-off sources and the consumers. A detailed investigation of the cartridge design remains necessary to assess the potential of this novel BOG recovery system. This study elaborates design concepts for the individual cartridge. A thorough material selection for suitable MH alloys is conducted and requirements for the cartridge design are derived. The key design features of the cartridges are determined and summarized in a morphological box. Four explicit design concepts are elaborated and illustrated. These results provide the baseline for upcoming studies to explicitly design and manufacture an MH cartridge demonstrator for testing, assisting the transformation to an even more sustainable LH2 industry.

Keywords: metal hydride; sustainable aviation; hydrogen; boil-off; conceptual design

1. Introduction

For decarbonizing the aviation sector, hydrogen presents a promising fuel option, especially in its liquid phase [1]. However, the inevitable formation of hydrogen boil-off gas (BOG) is a main drawback of liquid hydrogen (LH2) applications. As the venting of BOG reduces the overall efficiency and implies a safety risk at the airport, means for capturing and re-using the BOG should be implemented [2,3]. In addition to the significant undertaking of installing pipelines underneath the airport's apron to recover the boil-off losses, an infrastructure-independent system based on metal hydrides (MHs) presents an appealing alternative for aviation and beyond [4,5]. A particularly promising approach for MH-based BOG recovery is a system with exchangeable MH cartridges, which are used in a circulating manner. Although a previous study focuses on the macroscopic level of the interaction between the cartridges with the boil-off sources and potential consumers, a detailed investigation of the MH cartridge design remains necessary to assess the potential of this novel BOG recovery system and to prove its feasibility [6].

Academic Editors: Andreas Strohmayer, Spiros Pantelakis and Gustavo Alonso-Rodrigo

Received: 29 January 2026
Revised: 26 February 2026
Accepted: 2 March 2026
Published: 4 March 2026

Hence, this study elaborates design concepts for the MH cartridges to be used for BOG recovery. Firstly, the state of the art of MH cartridges for boil-off recovery is presented. Secondly, the methodology of the conceptual design process is described. Subsequently, the process is started by deriving the requirements. This step is supported by a systematic material selection and by analytical estimations of the acceptable MH bed thickness. A functional structure is then established and working principles are determined in a morphological box to identify the key design features. Finally, four explicit concepts are derived by the combination of these working principles. These concepts form the baseline for upcoming studies, in which a functional demonstrator is built that proves the feasibility of this novel approach of BOG recovery using exchangeable MH cartridges. This work is a revised and expanded version of a conference publication [7].

2. State of the Art of MH Cartridges for BOG Recovery

A previous study presents the macroscopic level of the MH-based BOG recovery system and briefly covers the MH cartridge regarding its shape and interfaces [6]. Hence, this current study focuses on the cartridge design as contextualized in Figure 1. The exchangeable MH cartridges consist of the following components [8,9]:

- A gas-proof vessel, in which the MH material is placed;
- Inputs and outputs for the heat transfer fluid (HTF) to supply or remove the heat of the reaction;
- Means for the input, output and distribution of hydrogen.

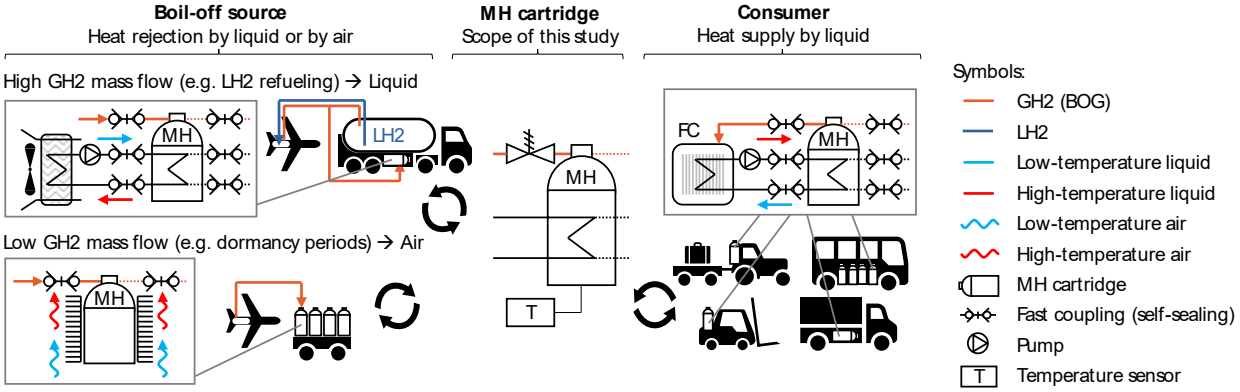

Figure 1. Overview of the MH-based boil-off recovery system to illustrate the scope of the conceptual design of this study based on [6].

The cartridges can be filled with hydrogen from various boil-off sources. While a liquid HTF is required to reject the heat of absorption at high hydrogen mass flow rates, the cooling by ambient air may be sufficient at lower rates [6]. For the subsequent hydrogen extraction and delivery to a consumer, the supply of waste heat for the desorption reaction is reasonable with a liquid HTF.

Hampton et al. experimentally investigated the capture of boil-off hydrogen with La-Ni alloys and thereby demonstrated general material suitability [10]. Explicit cartridge designs for the capture, recovery or pressurization of BOG from LH2 storage by MHs or any other solid hydrogen storage material have been presented by other studies [11,12]. Combinations of explicit cartridge designs with experimental validation are published as well [4,13–15]. Fuura et al. experimentally investigated the MH-based on-board capture of boil-off losses that result over time from heat leakage into the LH2 tank of a vehicle, for example during parking periods [14]. Although the MH cartridge offers internal HTF channels to provide the heat for desorption from a fuel cell (FC), cooling by natural convec-

tion with ambient air is sufficient for absorption due to the relatively low hydrogen mass flow rates. The design of the internal structure of the cartridge is not displayed. Neither is it explored what hydrogen mass flow rates could be achieved by using the internal HTF channels for dissipating the heat of absorption. In another study, Rosso and Golben [4] demonstrated the rapid absorption of low-pressure GH2 to validate the suitability of MHs for BOG capture from LH2 refueling operations. They achieved absorption durations of less than 10 min using forced liquid cooling. However, their coil-shaped design is not favorable for exchangeable MH cartridges that are to be used in a circulating manner. Based on this successful cartridge design, further design concepts will be elaborated in this study for the purpose of meeting the requirements of the previously proposed BOG recovery system like compactness and exchangeability [6].

3. Methodology for the Conceptual Design of the MH Cartridge

The process for the conceptual design of the MH cartridge is adopted from the previous study of the MH-based BOG recovery system [6]. Figure 2 illustrates the process while the following section presents the results of its steps.

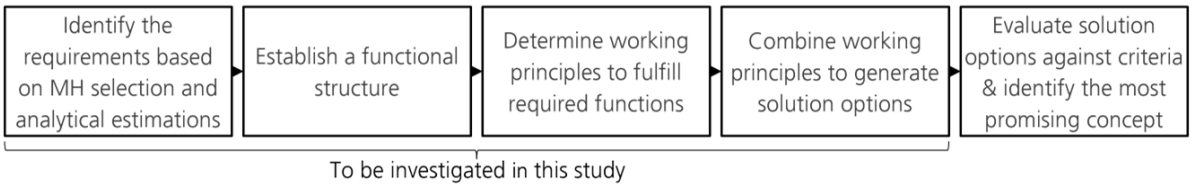

Figure 2. Process steps of the conceptual design adopted from [6].

4. Results of the Conceptual Design

4.1. Requirements and Material-Based Estimations

The conceptual design of the cartridge adopts the requirements from the previous system-level study [6], which will be described in thisparagraph. During absorption, the ambient air shall serve as the heat sink to reject the heat of the reaction. To enable the absorption of high BOG mass flow rates from LH2 refueling operations, the MH cartridge should include means for a liquid HTF to dissipate the generated heat to the heat sink as depicted in Figure 1. In addition, the cartridge should allow for a connection to external fins for air cooling, which could reduce infrastructure and power supply demands at low hydrogen boil-off rates. To drive the desorption reaction for supplying the captured BOG to an FC-powered consumer, the waste heat of the FC is provided to the MH material by the HTF. This results in operational requirements, which are summarized as design points in Table 1. The composition of the BOG is considered to be pure hydrogen with a high purity grade as it is formed by vaporization of LH2. Apart from this pure hydrogen BOG, BOG containing a mixture of hydrogen and helium is also produced during refueling operations because the LH2 systems and lines are filled with helium when not in service and have to be purged with hydrogen before usage [16]. However, the suitability of La-Ni alloys for the purification of such helium and hydrogen mixtures has already been successfully demonstrated by Hampton et al. [10].

Table 1. Design point parameter definition partly based on previous system-level study [6].

Parameter	Value	Comments
Target absorption time t_{abs}	30 min	LH2 refueling time [3,4,17]
Target desorption time t_{des}	180 min	Assumption
Target absorption pressure p_{abs}	≥1.2 bar	LH2 tank pressure as BOG pressure [2,3]
Target desorption pressure p_{des}	≥2 bar	FC inlet pressure [18]
Temperature to reject heat during absorption $T_{HTF,abs}$	≤39.4 °C	Aerospace standard hot day [19]
Temperature to drive desorption $T_{HTF,des}$	≤80–100 °C	Waste heat of LT-PEMFC [20]

Expected challenges for the conceptual design that arise from these design points are as follows:

- The relatively short absorption time, which requires high heat transfer rates and causes higher hydrogen pressure losses;
- The desired pressure elevation from absorption to desorption;
- The relatively high heat rejection temperature for absorption;
- The narrow temperature difference between absorption and desorption.

To contextualize these expected challenges, the MH material-specific behavior is described in the following sub-section.

4.1.1. Selection of a Suitable MH Alloy

The identification of a suitable MH alloy is usually assisted by van't Hoff plots of an array of different alloys [5,21]. A generic van't Hoff plot is illustrated in Figure 3 on the left-hand side. The material-specific pressure–temperature correlation of the MH's equilibrium condition, which resembles a straight line in this van't Hoff plot, has to lie in between the design points of absorption and desorption [22]. When comparing the van't Hoff plots of multiple alloys, only a single line for each alloy is often illustrated as a simplification. However, the following two properties also need to be considered: the plateau slope of the equilibrium condition and the hysteresis between absorption and desorption, including the deviations for the dynamic hysteresis behavior [4,22]. The van't Hoff plots are derived from the pressure–concentration isotherms (PCIs) of isothermal experiments as illustrated in Figure 3.

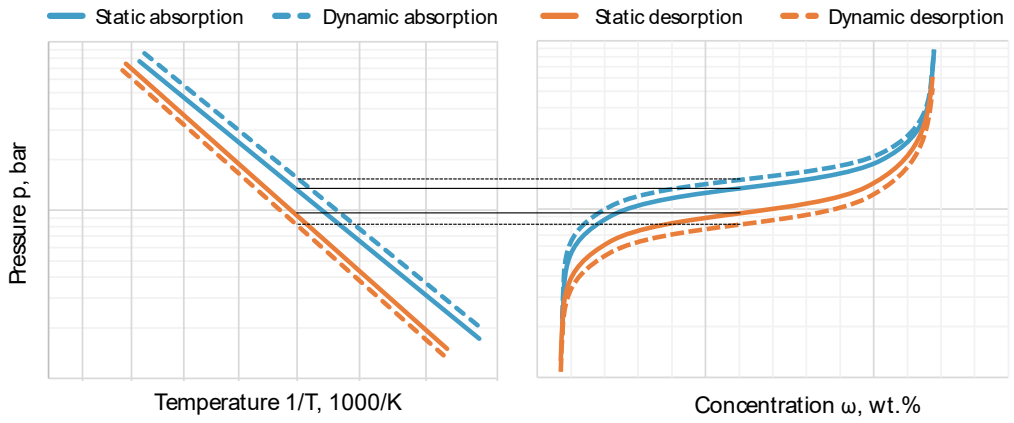

Figure 3. Exemplary comparison of the van't Hoff plot on the left and corresponding pressure–concentration isotherms (PCIs) on the right for a generic alloy.

These graphs of a generic MH alloy show the deviation of the van't Hoff plot caused by hysteresis and by dynamic operation. When the mid-plateau pressures are used to interpolate the van't Hoff plots as illustrated in Figure 3, an additional margin between the operating points and these plots needs to be considered. To achieve a high concentration

during absorption and a low concentration during desorption, an even higher or respectively lower operating pressure is required to compensate the plateau slope of the PCIs. Hence, after identifying a potentially suitable alloy, the specific PCIs of the design points have to be taken into account.

Figure 4a provides an overview of potential alloys for boil-off recovery. By inserting the data from Table 1, the alloy LaNi4.6Al0.4 is identified as a promising alloy, as its van't Hoff plot lies in between the design points. However, the specific PCIs of the alloy are additionally illustrated in Figure 4b so that the aforementioned properties of plateau slope, hysteresis and dynamic behavior can be considered. Due to the relatively short target absorption time t_{abs} of 30 min, a dynamic PCI is utilized to represent the absorption behavior while a static PCI is applied for desorption. It has to be noted that the PCI for absorption refers to a temperature of 25 °C, which is below the maximum target temperature $T_{HTF,abs}$ from Table 1. The reasons for selecting a lower absorption temperature are the lack of data on the one hand and the goal to achieve a high usable conversion on the other hand. The usable conversion describes the difference in the maximum gravimetric concentration of hydrogen in the alloy that can be achieved during absorption and the minimum concentration that can be achieved during desorption. The target pressures from Table 1 and the PCI temperatures used in Figure 4b allow for the favorable operation of the chosen alloy in the range of its plateau regions. This enables a usable hydrogen conversion ω_{max} of approximately 1 wt.%. Although Figure 4a,b indicate the general suitability of LaNi4.6Al0.4, the provided data is not sufficient for a detailed cartridge design. For future studies, dedicated experiments are recommended to generate PCI data of the designated MH alloy for the actual hydrogen mass flow rates and pressure levels of the design points of the target application from Table 1.

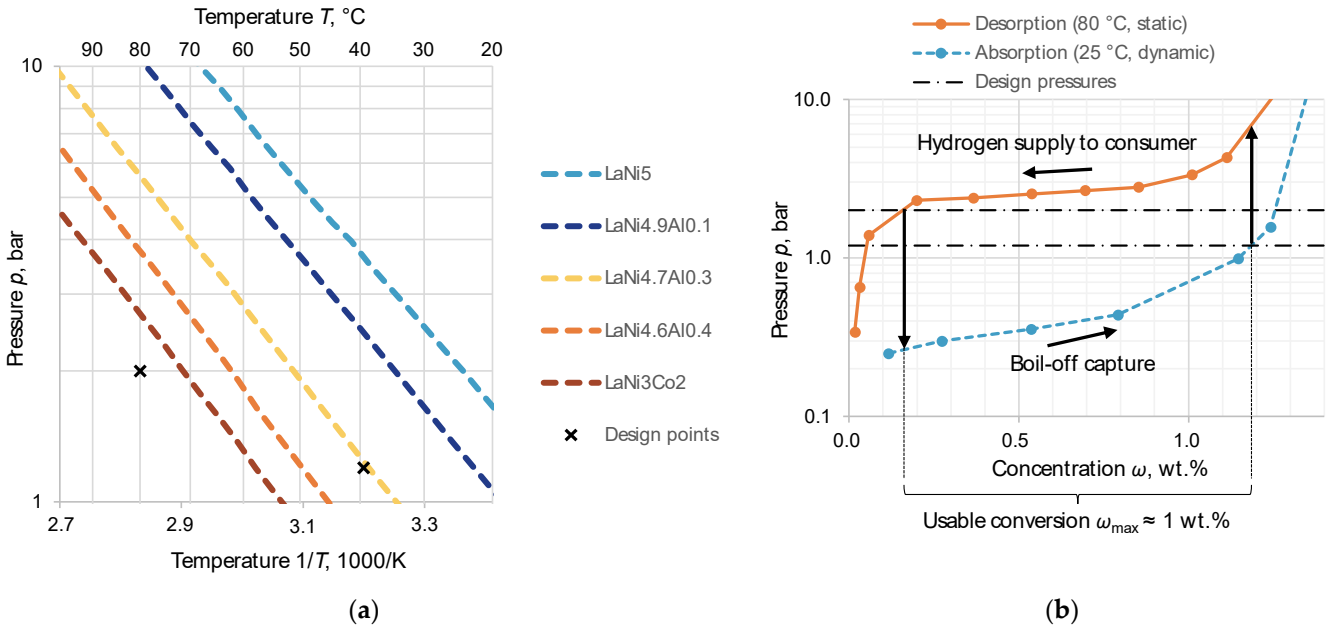

Figure 4. Illustration of the design points for alloy selection based on data from [4]: (**a**) van't Hoff plots of various alloys showing potential suitability of LaNi4.6Al0.4; (**b**) pressure–concentration isotherms (PCIs) of LaNi4.6Al0.4 with estimation of usable conversion.

However, as the design pressures are close to the plateau regions, any pressure loss and any temperature derivation within the MH cartridge would directly reduce the usable conversion. Hence, a low pressure and temperature gradient are key parameters for the MH cartridge design as already highlighted by Yang et al. and by Kölbig et al. [22,23]. As the MH bed is a kind of porous medium and contributes significantly to the aforementioned

gradients, the reductions in the thermal transfer distance and in the GH2 travel distance through the MH bed are fundamental [22,23].

4.1.2. Analytical Estimation of MH Bed Thickness

To examine the demand for design features to enhance the transfer of heat and the transport hydrogen gas, the acceptable MH bed thickness is estimated in relation to a given limit for the temperature gradient ΔT and to a given limit for the pressure drop Δp. This section starts with the estimations regarding the heat transfer limitations and their resulting temperature gradients. The heat of reaction $\dot{Q}$ can be calculated with the molar mass flow of hydrogen $\dot{n}_{H2}$ and the reaction enthalpy ΔH as follows [24,25]:

$$\dot{Q} = \dot{n}_{H2} \cdot \Delta H = \dot{m}_{H2} \cdot \frac{\Delta H}{M_{H2}}. \quad (1)$$

The variables $\dot{m}_{H2}$ and M_{H2} represent the mass flow rate and the molar mass of hydrogen. While the heat of reaction $\dot{Q}$ needs to be rejected from the MH bed during absorption, the supply of $\dot{Q}$ is required to engender the desorption. Within the MH cartridge, the heat is transferred from the MH bed to the HTF or vice versa. The thermal heat flux P within the MH cartridge can be described as follows [6,22,26]:

$$P = U_{total} \cdot A \cdot \Delta T = U_{total} \cdot A \cdot (T_{HTF} - T_{MH}) \text{ with} \quad (2)$$

$$U_{total} = \frac{1}{R_{total}} \text{ and} \quad (3)$$

$$R_{total} = \frac{s_{MH}}{\lambda_{MH}} + \frac{1}{\alpha_{wall}} + \frac{s_{wall}}{\lambda_{wall}} + \frac{1}{\alpha_{HTF}}. \quad (4)$$

Factor A describes the available area for heat transfer and indicates the importance of a high surface-to-volume ratio. The variables s and λ are the travel distance through the solid layers of the MH cartridge and their corresponding thermal conductivity. The variable α represents the heat transfer coefficients between the cartridge wall and its adjacent layers. The layers and their corresponding variables are illustrated in Figure 5, which shows a schematic cross section resembling a unit cell of an MH cartridge.

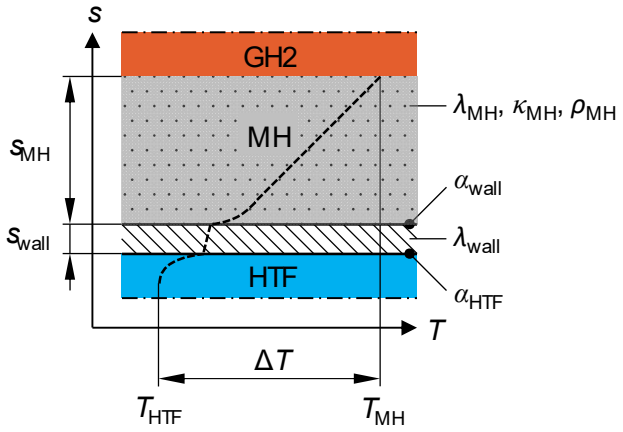

Figure 5. Schematic of a unit cell of the MH cartridge to illustrate the heat transfer path including the exemplary temperature distribution during absorption based on [22,27].

To calculate an average heat of reaction $\dot{Q}$, the average hydrogen mass flow rate $\dot{m}_{H2}$ is derived with the following equations [18]:

$$\dot{m}_{H2} = \frac{m_{H2}}{t} \text{ with} \quad (5)$$

$$m_{H2} = m_{MH} \cdot \omega_{max} = V_{MH} \cdot \rho_{MH} \cdot \omega_{max}. \quad (6)$$

The variables m_{MH}, V_{MH} and ρ_{MH} represent the mass, volume and volumetric mass density of the unit cell of the MH cartridge. The abbreviations of the indices can also be found in the list of abbreviations at the end of this manuscript. The time t embodies either the target absorption time t_{abs} or the target desorption time t_{des}. Combining Equation (1) with (5) and (6) delivers Equation (7):

$$\dot{Q} = \dot{m}_{H2} \cdot \frac{\Delta H}{M_{H2}} = \frac{V_{MH} \cdot \rho_{MH} \cdot \omega_{max} \cdot \Delta H}{t \cdot M_{H2}}. \quad (7)$$

By inserting the dimensions of the unit cell, the average heat of reaction $\dot{Q}$ of the unit cell can be calculated as follows:

$$\dot{Q} = \frac{s_{MH} \cdot A \cdot \rho_{MH} \cdot \omega_{max} \cdot \Delta H}{t \cdot M_{H2}}. \quad (8)$$

In an idealistic scenario, the MH should be kept in an isothermal condition during absorption and desorption so that the reaction rate is not deteriorated by heating up or cooling down [6]. Therefore, the heat flux P has to be equal to the heat of reaction $\dot{Q}$ as shown in Equation (9). By accordingly setting Equation (2) equal to Equation (8), the area A can be eliminated as shown in Equation (10):

$$\dot{Q} = P, \quad (9)$$

$$\frac{s_{MH} \cdot \rho_{MH} \cdot \omega_{max} \cdot \Delta H}{t \cdot M_{H2}} = \frac{\Delta T}{\frac{s_{MH}}{\lambda_{MH}} + \frac{1}{\alpha_{wall}} + \frac{s_{wall}}{\lambda_{wall}} + \frac{1}{\alpha_{HTF}}}. \quad (10)$$

Subsequently, Equation (10) is converted into the quadratic Equation (11), which can be solved with the quadratic formula to estimate the acceptable MH bed thickness s_{MH} for a given temperature gradient ΔT as shown in Equation (12):

$$0 = {s_{MH}}^2 + \left(\frac{\lambda_{MH}}{\alpha_{wall}} + \frac{s_{wall} \cdot \lambda_{MH}}{\lambda_{wall}} + \frac{\lambda_{MH}}{\alpha_{HTF}} \right) s_{MH} - \frac{\Delta T \cdot t \cdot M_{H2} \cdot \lambda_{MH}}{\rho_{MH} \cdot \omega_{max} \cdot \Delta H}, \quad (11)$$

$$s_{MH} = -\left(\frac{\lambda_{MH}}{2 \cdot \alpha_{wall}} + \frac{s_{wall} \cdot \lambda_{MH}}{2 \cdot \lambda_{wall}} + \frac{\lambda_{MH}}{2 \cdot \alpha_{HTF}} \right) \pm \left(\left(\frac{\lambda_{MH}}{2 \cdot \alpha_{wall}} + \frac{s_{wall} \cdot \lambda_{MH}}{2 \cdot \lambda_{wall}} + \frac{\lambda_{MH}}{2 \cdot \alpha_{HTF}} \right)^2 + \frac{\Delta T \cdot t \cdot M_{H2} \cdot \lambda_{MH}}{\rho_{MH} \cdot \omega_{max} \cdot \Delta H} \right)^{\frac{1}{2}}. \quad (12)$$

As a negative MH bed thickness is not reasonable, only the form of Equation (12) with the plus sign delivers a valid solution. It has to be noted that the argumentation from above is an idealistic scenario and underlies the following assumptions: steady-state conditions, a uniform temperature distribution in the MH bed and heat transfer only in thickness direction within the unit cell. This resembles a simplification of the real reaction behavior of the MH, which will be transient and spatially non-uniform [28,29]. In addition to these assumptions, the energy to heat up the BOG is not considered as its temperature depends on the final system setup in terms of the length of the lines and their insulation. However, neglecting the heat uptake of the BOG leads to conservative results as this reduces the heat energy that has to be dissipated by the HTF during absorption.

To estimate the acceptable MH bed thickness in relation to gas transport limitations and its corresponding pressure drop, Darcy's equation for the flow through porous media according to Equation (13) is used [23,30,31]:

$$\frac{\dot{V}_{H2}}{A} = \frac{\kappa \cdot \Delta p}{\mu_{H2} \cdot s_{MH}} \text{ with} \quad (13)$$

$$\dot{V}_{H2} = \frac{\dot{m}_{H2}}{\rho_{H2}}. \tag{14}$$

While $\dot{V}_{H2}$ is the volumetric flow rate of hydrogen, the variable μ_{H2} represents its viscosity. The permeability of the MH bed is described by κ_{MH}. With Equations (5) and (6), Equation (13) is converted to Equation (15):

$$\frac{\dot{m}_{H2}}{A \cdot \rho_{H2}} = \frac{m_{H2}}{A \cdot \rho_{H2} \cdot t} = \frac{V_{MH} \cdot \rho_{MH} \cdot \omega_{max}}{A \cdot \rho_{H2} \cdot t} = \frac{s_{MH} \cdot \rho_{MH} \cdot \omega_{max}}{\rho_{H2} \cdot t} = \frac{\kappa \cdot \Delta p}{\mu_{H2} \cdot s_{MH}}. \tag{15}$$

Rearranging Equation (15) for s_{MH} leads to Equation (16), which allows the acceptable MH bed thickness for a given pressure drop Δp to be estimated:

$$s_{MH} = \sqrt{\frac{\kappa \cdot \Delta p \cdot \rho_{H2} \cdot t}{\mu_{H2} \cdot \rho_{MH} \cdot \omega_{max}}}. \tag{16}$$

These argumentations for the gas transport also have underlying assumptions, which are named as follows: steady-state conditions, a uniform temperature distribution in the MH bed, constant hydrogen properties and gas transport only in the thickness direction of the unit cell.

To estimate an acceptable MH bed thickness as a guidance for the conceptual design, the input parameters of Tables 1 and 2 are used in Equations (12) and (16). The density of hydrogen ρ_{H2} results from the ideal gas equation according to Equations (17) and (18) [32]:

$$p \cdot V = m \cdot R \cdot T \; or \tag{17}$$

$$\rho_{H2} = \frac{p}{R_{H2} \cdot T}. \tag{18}$$

Table 2. Assumptions for the estimation of an acceptable MH bed thickness.

Parameter	Value	Source
Thermal conductivity of MH bed λ_{MH}	Powder: 1 W m^{-1} K^{-1}; compacts with ENG or powder with conductive elements: 10 W m^{-1} K^{-1}	[33–35]
Thermal conductivity of wall λ_{wall}	Aluminum alloy: 155 W m^{-1} K^{-1}	[33,36]
Heat transfer coefficient between MH and wall α_{wall}	1000 W m^{-2} K^{-1}	[37–39]
Heat transfer coefficient between wall and HTF α_{HTF}	400–6000 W m^{-2} K^{-1} with chosen value of 1000 W m^{-2} K^{-1}	[37,38,40,41]
Reaction enthalpy ΔH of LaNi4.6Al0.4	34.6 kJ mol^{-1}	[42]
Density of MH bulk material based on LaNi4.7Al0.3	7440 kg m^{-3}	[34]
Density of MH bed ρ_{MH}	Powder: 2445 kg m^{-3} based on porosity of 67% Compacts: 5208 kg m^{-3} based on porosity of 30%	[25,43]
Permeability of MH bed κ_{MH}	Powder: 1.75 × 10^{-13} m^2; compacts: 1.5 × 10^{-15} m^2	[33,41]
Hydrogen viscosity μ_{H2}	Linearly scaled from 0.84 × 10^{-5} Pa s at 0 °C to 1.04 × 10^{-5} Pa s at 100 °C	[13,44]
Special gas constant of hydrogen R_{H2}	4124.4 J kg^{-1} K^{-1}	[32]
Temperature gradient ΔT	5 K	Target
Pressure drop Δp	0.1 bar	Target
Usable conversion ω_{max}	1 wt.%	Target
Wall thickness s_{wall}	1 mm	Assumption

As the density of hydrogen ρ_{H2} is affected by pressure and temperature according to Equation (18), the above-mentioned assumptions lead to deviations between the calculated density of hydrogen and the actual local densities within the MH bed. Consequently, the result of Equation (16) is also affected and should therefore rather be seen as an estimation for the conceptual design rather than a binding sizing operation of the MH bed thickness.

The MH can be used in its delivery state as a powder or in compressed form as compacts [6]. The compacts offer several advantages such as a lower susceptibility to particle disintegration and accumulation, and their increased thermal conductivity by an order of magnitude compared to powder as stated in Table 2 [23]. The latter will enable a higher acceptable MH bed thickness in the heat transfer direction. However, compacts limit the design possibilities of the cartridge and they suffer from a lower permeability by two orders of magnitude as seen in Table 2 as well [22,45]. The latter will reduce the acceptable MH bed thickness in the direction of the gas transport compared to MH powder.

The results of the calculations are summarized in Table 3. By using MH powder, the acceptable MH bed thickness in the heat transfer direction is 3.6 mm to achieve the temperature gradient target. The acceptable MH bed thickness in the direction of the gas transport is 36.1 mm to attain the pressure drop target. In contrast to the illustration of the unit cell in Figure 5, the heat transfer direction and the gas transport path may not be aligned in the same direction. The direction of the heat transfer can be oriented perpendicular or at any other angle to the gas transport as the channels for HTF and hydrogen gas may be oriented in different dimensions of the three-dimensional design space. According to the results for MH powder, the acceptable MH bed thickness in the direction of the gas transport is an order of magnitude higher than in the heat transfer direction. Hence, the cartridge design may incorporate ten times as many HTF channels as gas channels. To avoid spatial conflicts and to not introduce more gas channels than are necessary, it may be advisable to arrange the different channels vertically to each other.

Table 3. Results of the estimation of the MH bed thickness as an input for necessary design features to enhance the transfer of heat and the transport hydrogen gas for the conceptual design.

Input for Calculation	**Acceptable MH Bed Thickness Value**	
	MH Powder	**MH Compact**
Temperature gradient calculation according to Equation (12):		
Absorption conditions	3.6 mm	7.4 mm
Desorption conditions	10.1 mm	26.3 mm
Pressure drop calculation according to Equation (16):		
Absorption conditions	36.1 mm	2.3 mm
Desorption conditions *	98.1 mm	6.2 mm

* Desorption temperature of 100 °C from Table 1 applied as this leads to conservative lower values for the MH bed thickness.

For MH compacts, the acceptable MH bed thickness is 7.4 mm in the heat transfer direction and 2.3 mm in the direction of the gas transport. These results underline the demand for a narrow MH bed thickness as a requirement for the cartridge design.

4.2. Functional Structure Tree

The functional structure of the MH cartridge is derived from the requirements and from the previous study of the BOG recovery system [6]. The result is illustrated as a functional structure tree in Figure 6.

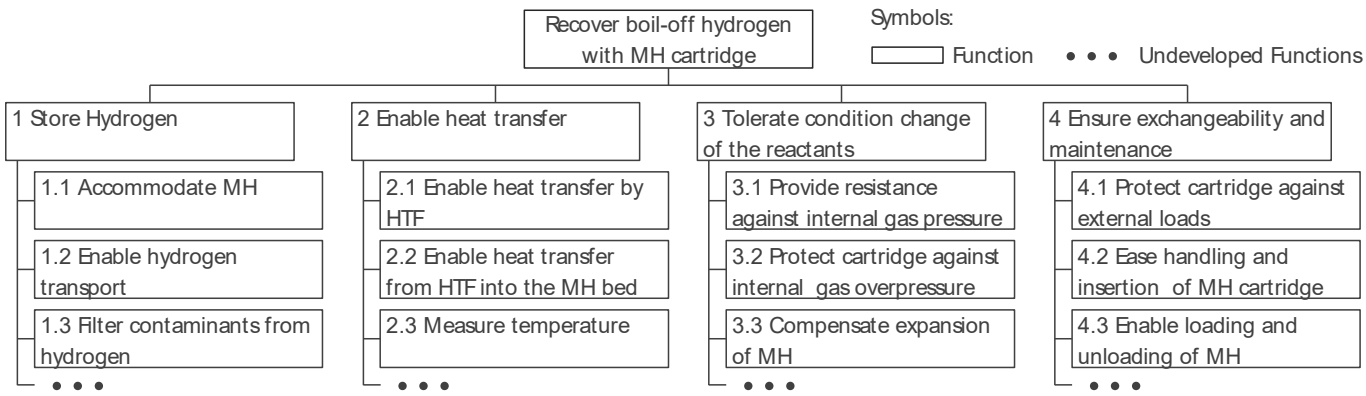

Figure 6. Functional structure tree of the MH cartridge.

4.3. Working Principles

In this next step of the conceptual design process, working principles for the various functions are elaborated from literature research on the one hand and from brainstorming sessions with people from different engineering fields on the other hand. The working principles are compiled as a morphological box in Table 4, which is guided by previous conceptual designs [6,46,47].

The working principles may be specified in more detail during the further refinement of the design. For example, the HTF channels of working principle A for function 2.1 can be realized with different cross-section shapes. The channels can also follow different paths through the cartridge, e.g., a longitudinal, radial or transversal course or even combinations thereof resulting in zigzag-, spiral- or grid-shaped courses [46]. It should also be noted that apart from the compiled solutions for function 3.3, the impact of MH expansion can also be reduced by limiting the initial filling fraction to 40 % or by re-cycling the MH before filling [22,23].

4.4. Combination of Working Principles to Concepts

To develop conceptual designs that fulfill the primary function 'Recover boil-off hydrogen with MH cartridge', it is necessary to combine the working principles of each of the single functions to create solution options [48]. The scheme of the morphological box according to Table 4 is particularly suited for systematically deriving solution options. It should be emphasized that this process step is intended to lead to several solution variants and that only those working principles that are compatible should be combined. Four exemplary concepts, which are derived from the morphological box, are presented in the following sub-sections: plate-fin concept, gyroid concept, dendrite concept and tube-bundle concept. These four concepts resemble pertinent options toward a feasible MH cartridge design, although they should not be understood as all-encompassing as other combinations may also be reasonable. The combination logic is driven by defining a main motivation for each concept and then adding promising working principles.

Table 4. Morphological box for the conceptual design of the metal hydride cartridge.

ID	Function	Working Principle A	Working Principle B	Working Principle C
1.1	Accommodate MH	Cylindrical MH vessel	Prismatic MH vessel	Coil-shaped MH vessel
1.2	Enable GH2 transport	Ullage above MH bed	Hydrogen artery [6,23]	Short travel length in MH bed
1.3	Filter contaminants	Filter in interface [33]	Filter end cap [49]	Filter as GH2 artery [50–52]

Table 4. *Cont.*

ID	Function	Working Principle A	Working Principle B	Working Principle C
2.1	Enable heat transfer by HTF	Internal channels (e.g., straight or helical tubes)	Heat exchanger plates as separate components	External jacket
2.2	Enable heat transfer from HTF into the MH bed	Conductive matrices (e.g., metal foam, fins, honeycombs, pins, dendrites or TPMS) [46,53]	Admixture of thermal conductive material (e.g., ENG, graphite fibers, and aluminum particles) [6,54]	MH compacts [6]
2.3	Measure temperature	Temperature sensor at the vessel surface	Temperature sensor in MH bed	External temperature sensor in HTF return pipe
3.1	Provide resistance against gas pressure	Sufficient strength of vessel structure [46]	Implementation of internal braces as reinforcement [46]	Implementation of external stiffeners as reinforcement
3.2	Protect cartridge against overpressure	Non-reclosing pressure relief device (such as rupture disks or diaphragms) [55]	Re-sealable pressure relief device (such as pressure relief valves) [55]	
3.3	Compensate expansion of MH	Admixture of additives (e.g., ENG) [6,56]	Prevent local accumulation of MH by reduction in vertical height or by dividers [23]	Flexible design (e.g., springs, elastic sheets or deformable vessel) [13,23,33]
4.1	Protect cartridge against external loads	Elastic bumper devices [6]	Rigid casings	Protective collar to shield the interfaces
4.2	Ease handling and insertion of cartridge	Handles, lugs or threads for lifting [6]	Guide rails or guide pins for insertion [6]	Wheels [6]
4.3	Enable loading and unloading of MH	Re-sealable ports	Removable side face	Dismantling of vessel

4.4.1. Plate-Fin Concept

The plate-fin concept is a stacked assembly of prismatic MH vessels and planar HTF channels as shown in Figure 7. The MH powder is arranged between fins that are connected to the HTF channels. Besides transferring the heat, the fins also serve as internal braces to reinforce the vessel structure against the internal gas pressure. Moreover, the fins reduce the vertical MH bed height to prevent accumulation of MH powder at the bottom of the cartridge. The main motivation for this concept is to decouple the heat transfer and gas transport directions. The fins split the MH bed into narrow layers with heat transfer in the thickness direction. As the gas transport distance through the MH can be an order of magnitude longer according to Table 3, the gas is transported in the plane of this layer. The use of simple parts and the scalable and compact design are advantages of this concept. Disadvantages could be the long gas transport distance, which contributes to hydrogen pressure drop, and the high number of interfaces, which increase complexity and are prone to leakage.

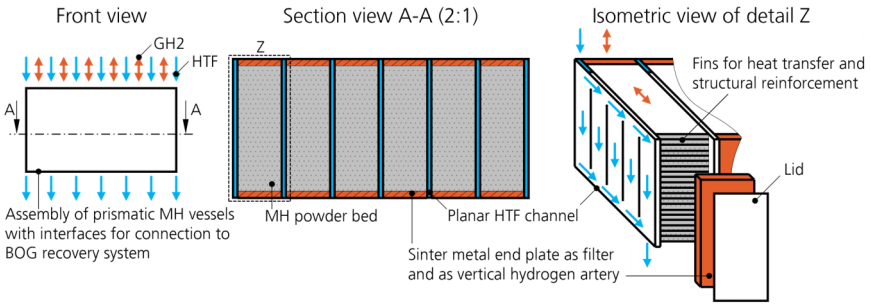

Figure 7. Plate-fin concept—Prismatic stack with fins and planar HTF channels.

4.4.2. Gyroid Concept

The gyroid concept exhibits a prismatic outer shape as well. But in contrast to the planar fins of the plate-fin concept, the MH powder is now filled into a strongly curved gyroid-type triply periodic minimal surface (TPMS) structure as illustrated in Figure 8. This TMPS structure not only provides a high surface area for heat transfer, which is the main motivation for this concept, but is also equipped with integrated HTF channels as proposed by Sain et al. [57]. The advantages of the gyroid concept are the low number of interfaces, the high heat transfer area and the compact design. As a potential drawback, the production of the cartridge requires additive manufacturing techniques. Moreover, the vessel needs to be flat in shape to limit the gas transport distance through the MH bed and to prevent accumulation of MH powder at the bottom.

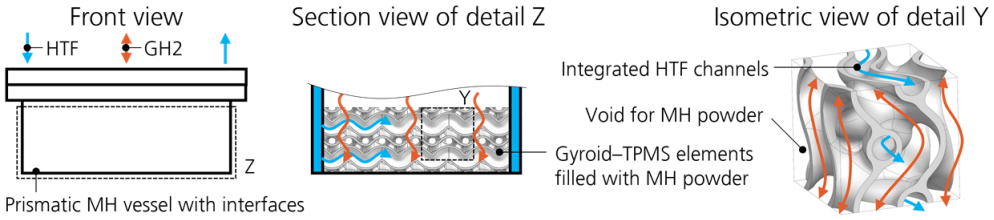

Figure 8. Gyroid concept—Prismatic vessel with gyroid-type TPMS structure.

4.4.3. Dendrite Concept

In contrast to the previous concepts, the dendrite concept is based on a cylindrical vessel that contains all cartridge components, like the HTF channels or the dendrite-shaped conductive elements. As depicted in Figure 9, the HTF channels are arranged in the longitudinal direction of the vessel. Sinter metal plates are placed in the radial direction in such a way that a free space is formed in the center of the cartridge as a passage for the GH2 in longitudinal direction.

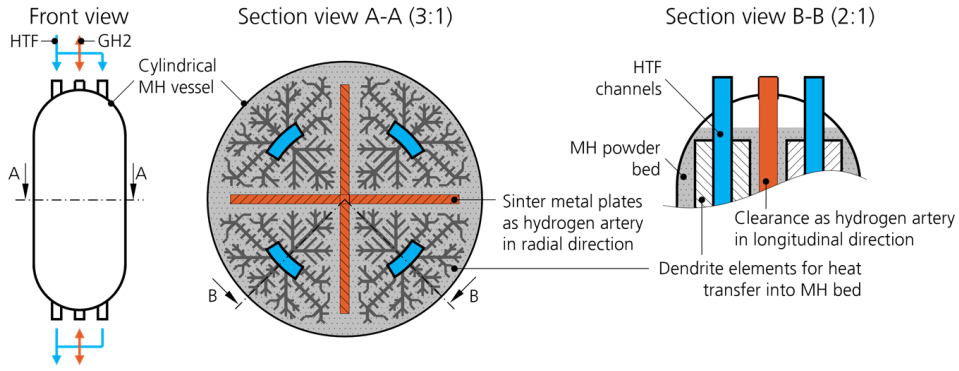

Figure 9. Dendrite concept—Cylindrical vessel with dendrite elements.

The main motivation of the dendrite concept is the inherent strength of the cylindrical vessel against internal pressure, which allows for higher absorption and desorption pressures without significantly increasing the passive reactor mass. The dendrite elements ensure a short heat transfer distance through the MH bed. However, the cylindrical vessel impairs the filling of the MH material, the assembly of the components and the handling of the cartridge. The illustrated design is also prone to MH accumulation at the bottom of the cartridge, which may be reduced by operating the cartridge in a horizontal position.

4.4.4. Tube-Bundle Concept

In contrast to the previous concepts, the tube-bundle concept according to Figure 10 is the only concept using MH compacts. The disk-shape compacts are stacked in cylindrical vessels together with sinter metal elements to reduce the gas transport path through the MH bed. The cylindrical MH vessels are arranged in a prismatic container. Thereby, the concept combines the structural strength of cylindrical vessels against internal pressure with a prismatic outer shape which is beneficial for handling and stacking of the cartridges. This combination of beneficial properties is the main motivation of this concept. The prismatic container is filled with HTF for immersion cooling and heating of the MH vessels. The tube-bundle concept makes use of semifinished parts, which are easy to manufacture, and allows for scaling of the total cartridge size by increasing the number of cylindrical MH vessels within a prismatic container. Potential drawbacks are the complex assembly due to the high number of parts and the compactness deterioration due to the necessary sinter metal filter elements.

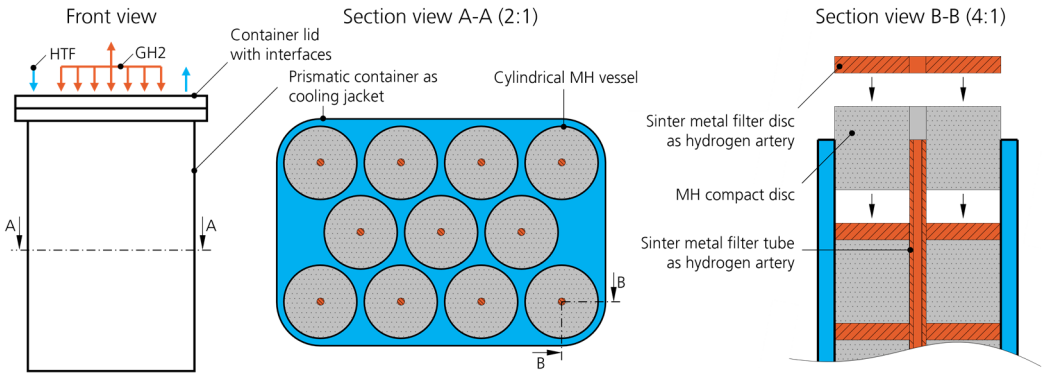

Figure 10. Tube-bundle concept—Multiple cylindrical vessels immersed in HTF.

4.4.5. Comparison of the Concepts

According to Figure 1, air cooling of the cartridge may be reasonable at low BOG mass flow rates. The plate-fin concept and the gyroid concept could be suitable for connecting the cartridge to external fins for direct heat rejection to the ambient air as proposed in the previous study [6]. While the flat shape of the gyroid concept seems beneficial for placing the whole cartridge between plates with external fins, the modular approach of the plate-fin concept allows for the replacement of the planar HTF channels with external fin elements.

For comparison of the four concepts, a balance of arguments is compiled in Table 5. The balance of arguments is a universally applicable approach for decision-making which is notable for its ease of implementation [58]. However, this approach is not suited to clearly identify the most promising concept as it lacks a numerical assessment by weighted criteria. Before selecting a concept by a numerical approach, the authors recommend elaborating a higher level of detail. For example, a sensitivity analysis of the analytical MH bed thickness estimation is proposed together with a sizing analysis of the HTF channels. The results of these analyses would enhance the numerical assessment of arguments and strengthen the concept selection regarding the relative feasibility.

Table 5. Balance of arguments to compare the advantages and disadvantages of the four concepts.

Plate-Fin Concept		**Gyroid Concept**		**Dendrite Concept**		**Tube-Bundle Concept**	
+	Compactness	+	Compactness	+	Inherent strength of vessel shape	+	Use of simple parts
+	Use of simple parts	+	Low number of parts and interfaces	+	Low number of parts and interfaces	+	Scalability
+	Scalability	+	High heat transfer area	−	Filling of MH material difficult	+	Inherent strength of vessel shape
+	Prevention of MH accumulation	+	Suited for air cooling by external fins	−	Difficult assembly	+	Outer shape simplifies handling and stacking
+	Suited for air cooling by external fins	+	Outer shape simplifies handling and stacking	−	Difficult handling	−	Complexity by high number of parts
+	Outer shape simplifies handling and stacking	−	Additive manufacturing required	−	Additional means for stacking required	−	Reduced compactness
−	Long gas transfer path	−	Limited to flat vessel shapes	−	Prone to MH accumulation	−	Low compatibility with external air cooling
−	Complexity by high number of parts and interfaces			−	Low compatibility with external air cooling		
−	Prone to leakage						

+ refers to arguments with a positive impact; − refers to arguments with a negative impact.

5. Conclusions

As previous studies already revealed the macroscopic level of the MH-based BOG recovery system, this current work conducts a conceptual design of the corresponding MH cartridges. First, the requirements were identified with support from a systematic MH alloy selection including material property considerations. Moreover, an analytical sizing guideline for the acceptable MH bed thickness was determined and conducted to generate input for the conceptual design. Subsequently, a functional structure tree was established before corresponding working principles were compiled in a morphological box. Finally, four specific concepts were elaborated and illustrated. The combination logic to derive these concepts was driven by defining a main motivation for each concept and then adding promising working principles from the morphological box. The concepts generate the baseline for upcoming studies to select a concept and to explicitly design a demonstrator of an MH cartridge for manufacturing and testing. Before selecting a concept, the conducted analytical estimations should be supplemented by a sensitivity analysis and by sizing of the necessary HTF channels. Moreover, dedicated experiments are recommended to generate PCI data of the designated MH alloy for the actual design point conditions. The results from these sensitivity, sizing and material investigations will enhance a numerical evaluation to identify the most promising concept to be pursued during the upcoming design of a demonstrator cartridge. The detailed demonstrator design should encompass mechanical and thermal simulations. The performance of the demonstrator should be validated by experiments to prove the feasibility of the cartridge design and to reveal its operational limits. Such experimental results would allow for a system-level assessment of the potential of MH-based boil-off recovery with exchangeable cartridges. If this assessment predicts promising potential, this novel approach of BOG recovery by MHs should be employed to full-scale demonstrators in a realistic environment. This encompasses not only the airport environment but also maritime infrastructures, spaceports and the automotive sector. Thereby, this novel approach could contribute not only to future sustainable aviation but also to the empowerment of LH2 as an energy carrier in general. Moreover, the established generic morphological box is also applicable for conceptual design studies of MH cartridges beyond BOG recovery.

Author Contributions: Conceptualization, F.F. and S.K.; methodology, F.F. and S.K.; formal analysis, F.F.; investigation, F.F.; writing—original draft preparation, F.F.; writing—review and editing, F.F. and S.K.; visualization, F.F. and S.K.; supervision, S.K.; project administration, F.F.; funding acquisition, F.F. and S.K. All authors have read and agreed to the published version of the manuscript.

Funding: This research received no external funding.

Data Availability Statement: The original contributions presented in the study are included in the article, further inquiries can be directed to the corresponding author.

Acknowledgments: We wish to acknowledge Lars Enghardt and Georg Pohl for their support in the investigation of boil-off recovery.

Conflicts of Interest: The authors declare no conflicts of interest.

Abbreviations

The following abbreviations are used in this manuscript:

BOG	Boil-off gas
ENG	Expanded natural graphite
FC	Fuel cell
GH2	Gaseous hydrogen
H2	Hydrogen
HTF	Heat transfer fluid
LH2	Liquid hydrogen
MH	Metal hydride
PCI	Pressure–concentration isotherm
TPMS	Triply periodic minimal surface

References

1. Baroutaji, A.; Wilberforce, T.; Ramadan, M.; Olabi, A.G. Comprehensive Investigation on Hydrogen and Fuel Cell Technology in the Aviation and Aerospace Sectors. *Renew. Sust. Energ. Rev.* **2019**, *106*, 31–40. [CrossRef]
2. Brewer, G.D. *Hydrogen Aircraft Technology*, 1st ed.; CRC Press LLC: Boca Raton, FL, USA, 1991.
3. Mangold, J.; Silberhorn, D.; Moebs, N.; Dzikus, N.; Hoelzen, J.; Zill, T.; Strohmayer, A. Refueling of LH2 Aircraft—Assessment of Turnaround Procedures and Aircraft Design Implication. *Energies* **2022**, *15*, 2475. [CrossRef]
4. Rosso, M.J.; Golben, P.M. *Capture of Liquid Hydrogen Boiloff with Metal Hydride Absorbers, NASA*; Ergenics Inc.: Ringwood, NJ, USA, 1984.
5. Franke, F.; Kazula, S.; Enghardt, L. Elaboration and Outlook for Metal Hydride Applications in Future Hydrogen-powered Aviation. *Aeronaut. J.* **2024**, *128*, 1501–1531. [CrossRef]
6. Franke, F.; Kazula, S. Conceptual Design of a Metal Hydride System for the Recovery of Gaseous Hydrogen Boil-off Losses from LH2 Tanks. *Aeronaut. J.* **2025**, *130*, 1–15. [CrossRef]
7. Franke, F.; Kazula, S. Conceptual Design of a Metal Hydride Cartridge for the Recovery of Gaseous Boil-off Losses from Liquid Hydrogen Tanks. In Proceedings of the 15th EASN International Conference, Madrid, Spain, 14–17 October 2025; ISBN 2673-4591.
8. Pohl, G. Konzeptentwicklung zum Auffangen und Verwerten von Gasförmigen Wasserstoffverlusten aus dem Boil-off von Flüssigwasserstofftanks Durch Metallhydrid. Bachelor's Thesis, BTU Cottbus-Senftenberg, Cottbus, Germany, 2024.
9. Lototskyy, M.V.; Tolj, I.; Pickering, L.; Sita, C.; Barbir, F.; Yartys, V. The Use of Metal Hydrides in Fuel Cell Applications. *Prog. Nat. Sci. Mater. Int.* **2017**, *27*, 3–20. [CrossRef]
10. Hampton, M.D.; Slattery, D.K.; Oztek, M.T. Alloys for Hydrogen Separation, Recovery and Purification. *Hydrog. Econ.* **2007**, *48*, 40–47.
11. Friedrich, T. Einrichtung zur Druckerhöhung für Wasserstoff. Espacenet DE 10 2005 004 590 A1, 1 February 2005.
12. Jaemyung, L.; Jinho, B.; Byeongkwan, H.; Seulkee, K.; Jeonghyeon, K. System for storing liquefied hydrogen and collecting boil-off hydrogen. Espacenet KR20200103404A, 25 February 2019.
13. Nakano, A.; Maeda, T.; Ito, H.; Masuda, M.; Kawakami, Y.; Tange, M.; Takahashi, T.; Nishida, K. Study on Absorption/Desorption Characteristics of a Metal Hydride Tank for Boil-off Gas from Liquid Hydrogen. *Int. J. Hydrogen Energy* **2012**, *37*, 5056–5062. [CrossRef]

14. Fuura, T.; Tsunokake, S.; Hirotani, R.; Hashimoto, T.; Akai, M.; Watanabe, S.; Enoki, H.; Akiba, E. Development of a LH2 Vehicle Tank Boil-off Gas Recovery System Using Hydrogen Storage Alloys. In Proceedings of the World Hydrogen Energy Conference, Yokohama, Japan, 27 June–2 July 2004.
15. Rosso, M.J.; Golben, P.M. Capture of Liquid Hydrogen Boil-off with Metal Hydride Absorbers. *J. Less-Common Met.* **1987**, *131*, 283–292. [CrossRef]
16. Oztek, M.T. Recovery of Hydrogen and Helium from Their Mixtures Using Metal Hydrides. Master's Thesis, University of Central Florida, Orlando, FL, USA, 2005.
17. Petitpas, G. Boil-Off Losses Along LH2 Pathway. LLNL-TR-750685, Lawrence Livermore National Laboratory, Livermore. 2018. Available online: https://www.osti.gov/servlets/purl/1466121 (accessed on 9 May 2023). [CrossRef]
18. Kölbig, M.; Bürger, I.; Linder, M. Characterization of Metal Hydrides for Thermal Applications in Vehicles below 0 °C. *Int. J. Hydrogen Energy* **2019**, *44*, 4878–4888. [CrossRef]
19. SAE. *Definition of Commonly Used Day Types; AS210*; SAE International: Warrendale, PA, USA, 2023.
20. U.S. Department of Transportation. Energy Supply Device Aviation Rulemaking Committee: Final Report. DOT/FAA/TC-19/16, Federal Aviation Administration, Springfield, Virginia 22161. 2017. Available online: https://www.faa.gov/regulations_policies/rulemaking/committees/documents/media/Energy%20Supply%20Device%20ARC%20Recommendation%20Report.pdf (accessed on 28 June 2022).
21. Bhuiya, M.M.H.; Kumar, A.; Kim, K.J. Metal Hydrides in Engineering Systems, Processes, and Devices: A Review of Non-storage Applications. *Int. J. Hydrogen Energy* **2015**, *40*, 2231–2247. [CrossRef]
22. Kölbig, M.; Weckerle, C.; Linder, M.; Bürger, I. Review on Thermal Applications for Metal Hydrides in Fuel Cell Vehicles: Operation Modes, Recent Developments and Crucial Design Aspects. *Renew. Sustain. Energy Rev.* **2022**, *162*, 112385. [CrossRef]
23. Yang, F.S.; Wang, G.X.; Zhang, Z.X.; Meng, X.Y.; Rudolph, V. Design of the Metal Hydride Reactors—A Review on the Key Technical Issues. *Int. J. Hydrogen Energy* **2010**, *35*, 3832–3840. [CrossRef]
24. Chabane, D.; Ibrahim, M.; Harel, F.; Djerdir, A.; Candusso, D.; Elkedim, O. Energy Management of a Thermally Coupled Fuel Cell System and Metal Hydride Tank. *Int. J. Hydrogen Energy* **2019**, *44*, 27553–27563. [CrossRef]
25. Weckerle, C.; Nasri, M.; Hegner, R.; Linder, M.; Bürger, I. A Metal Hydride Air-conditioning System for Fuel Cell Vehicles—Performance Investigations. *Appl. Energy* **2019**, *256*, 113957. [CrossRef]
26. VDI-Gesellschaft Verfahrenstechnik und Chemieingenieurwesen. (Ed.) *VDI Heat Atlas*, 2nd ed.; Springer: Berlin/Heidelberg, Germany, 2010.
27. Wenger, D. *Metallhydridspeicher zur Wasserstoffversorgung und Kühlung von Brennstoffzellenfahrzeugen*; TU München: München, Germany, 2009.
28. Zhuo, Y.; Jung, S.; Shen, Y. Numerical Study of Hydrogen Desorption in an Innovative Metal Hydride Hydrogen Storage Tank. *Energy Fuels* **2021**, *35*, 10908–10917. [CrossRef]
29. Nam, J.; Ko, J.; Ju, H. Three-dimensional Modeling and Simulation of Hydrogen Absorbtion in Metal Hydride Hydrogen Storage Vessels. *Appl. Energy* **2012**, *89*, 164–175. [CrossRef]
30. Sheng, J.J. *Enhanced Oil Recovery: Field Case Studies*; Gulf Professional Publishing: Oxford, UK, 2013.
31. Kam, S.I. Improved Mechanistic Foam Simulation with Foam Catastrophe Theory. *Colloids Surf. A Physicochem. Eng. Asp.* **2008**, *318*, 62–77. [CrossRef]
32. Klell, M.; Eichlseder, H.; Trattner, A. *Hydrogen in Automotive Engineering*; Springer Fachmedien: Wiesbaden, Germany, 2023.
33. Wimmer, A.; Kordel, M.; Linder, M.; Bürger, I. High Performance Reactor of a Metal Hydride Based Cooling System for Air-conditioning of Fuel Cell Electric Vehicles. *Appl. Energy* **2025**, *391*, 125911. [CrossRef]
34. Hahne, E.; Kallweit, J. Thermal Conductivity of Metal Hydride Materials for Storage of Hydrogen: Experimental Investigation. *Int. J. Hydrogen Energy* **1998**, *23*, 107–114. [CrossRef]
35. Nguyen, H.Q.; Shabani, B. Review of Metal Hydride Hydrogen Storage Thermal Management for Use in the Fuel Cell Systems. *Int. J. Hydrogen Energy* **2021**, *46*, 31699–31726. [CrossRef]
36. Sélo, R.R.; Catchpole-Smith, S.; Maskery, I.; Ashcroft, I.; Tuck, C. On the Thermal Conductivity of AlSi10Mg and Lattice Structures Made by Laser Powder Bed Fusion. *Addit. Manuf.* **2020**, *34*, 101214. [CrossRef]
37. Groll, M. Reaction Beds for Dry Sorption Machines. *Heat Recovery Syst. CHP* **1993**, *13*, 341–346. [CrossRef]
38. Klein, H.-P. Heat Transfer Characteristics of Expanded Graphite Matrices in Metal Hydride Beds. *Int. J. Hydrogen Energy* **2004**, *29*, 1503–1511. [CrossRef]
39. Pons, M.; Dantzer, P. Heat Transfer in Hydride Packed Beds. II. A New Experimental Technique and Results on LaNi5 Powder. *Z. Phys. Chem.* **1994**, *183*, 213–223. [CrossRef]
40. Dornheim, M.; Baetcke, L.; Akiba, E.; Ares, J.-R.; Autrey, T.; Barale, J.; Baricco, M.; Brooks, K.; Chalkiadakis, N.; Charbonnier, V.; et al. Research and Development of Hydrogen Carrier Based Solutions for Hydrogen Compression and Storage. *Prog. Energy* **2022**, *4*, 42005. [CrossRef]

41. Wimmer, A.; Linder, M.; Bürger, I. Metal Hydride-based Cooling System for Fuel Cell Electric Vehicles: Achieving a Temperature Lift of 40 K. *Appl. Energy* **2025**, *398*, 126396. [CrossRef]
42. Mendelsohn, M.H.; Gruen, D.M.; Dwight, A.E. The Effect of Aluminum Additions on the Structural and Hydrogen Absorption Properties of AB5 Alloys with Particular Reference to the LaNi5-xAlx Ternary Alloy System. *J. Less-Common Met.* **1979**, *63*, 193–207. [CrossRef]
43. Heubner, F.; Mauermann, S.; Kieback, B.; Röntzsch, L. Stress Development of Metal Hydride Composites for High Density Hydrogen Storage Applications. *J. Alloys Compd.* **2017**, *705*, 176–182. [CrossRef]
44. Engineering ToolBox. Gases—Dynamic Viscosities: Absolute (dynamic) Viscosities of Some Common Gases. Available online: https://www.engineeringtoolbox.com/gases-absolute-dynamic-viscosity-d_1888.html (accessed on 26 January 2026).
45. Payá, J.; Linder, M.; Mertz, R.; Corberán, J.M. Analysis and Optimization of a Metal Hydride Cooling System. *Int. J. Hydrogen Energy* **2011**, *36*, 920–930. [CrossRef]
46. Röver, T.; Roth, S.; Hoffmann, T.; Baetcke, L.; Herzog, D. *Development of a Hydrogen Metal Hydride Storage Produced by Additive Manufacturing*; EFCF: Lucerne, Switzerland, 2023.
47. Kretschmer, C. Entwicklung von Metallhydrid-Reaktoren mittels 3D-Druck und Charakterisierung Dieser für die Anwendung als Vorheizer in Einem Brennstoffzellenbetriebenem Lastenfahrrad. Master's Thesis, University of Stuttgart, Stuttgart, Germany, 2019.
48. Pahl, G.; Beitz, W.; Blessing, L.; Feldhusen, J.; Grote, K.-H.; Wallace, K. *Engineering Design: A Systematic Approach*, 3rd ed.; Springer: London, UK, 2007.
49. Lamberti, T. Dispositivo di unione e filtraggio per sistemi di stoccaggio del tipo ad idruri metallici a fascio tubiero. Espacenet IT 2022/00023775 A1, 17 November 2022.
50. Klein, H.-P.; Groll, M. Development of a Two-stage Metal Hydride System as Topping Cycle in Cascading Sorption Systems for Cold Generation. *Appl. Therm. Eng.* **2002**, *22*, 631–639. [CrossRef]
51. Muthukumar, P.; Prakashmaiya, M.; Srinivasamurthy, S. Experiments on a Metal Hydride Based Hydrogen Compressor. *Int. J. Hydrogen Energy* **2005**, *30*, 879–892. [CrossRef]
52. Gopal, M.; Murthy, S. Experiments on a Metal Hydride Cooling System Working With ZrMnFe/MmNi4.5Al0.5 Pair. *Int. J. Refrig.* **1999**, *22*, 137–149. [CrossRef]
53. Cui, Y.; Zeng, X.; Xiao, J.; Kou, H. The Comprehensive Review for Development of Heat Exchanger Configuration Design in Metal Hydride Bed. *Int. J. Hydrogen Energy* **2022**, *47*, 2461–2490. [CrossRef]
54. Muthukumar, P.; Kumar, A.; Raju, N.N.; Malleswararao, K.; Rahman, M.M. A Critical Review on Design Aspects and Developmental Status of Metal Hydride Based Thermal Machines. *Int. J. Hydrogen Energy* **2018**, *43*, 17753–17779. [CrossRef]
55. *ISO 16111*; Transportable Gas Storage Devices—Hydrogen Absorbed in Reversible Metal Hydride, 2nd ed. International Organization for Standardization: Geneva, Switzerland, 2018.
56. Lototskyy, M.; Tolj, I.; Klochko, Y.; Davids, M.W.; Swanepoel, D.; Linkov, V. Metal Hydride Hydrogen Storage Tank for Fuel Cell Utility Vehicles. *Int. J. Hydrogen Energy* **2020**, *45*, 7958–7967. [CrossRef]
57. Sain, C.K.; Mathiazhagan, A.; Bhapkar, S.; Kazula, S.; Asli, M.; Hoeschler, K. Design Assessment and Test of Compact Gyroid-TPMS Heat Exchanger with Embedded Coolant Channels for LTPEM Fuel Cell Powered Regional Aircraft. In Proceedings of the DLRK, Augsburg, Germany, 23–25 September 2025.
58. Feldhusen, J.; Grote, K.-H. *Pahl/Beitz Konstruktionslehre: Methoden und Anwendung Erfolgreicher Produktentwicklung*, 8th ed.; Springer: Berlin/Heidelberg, Germany, 2013.